Optimal design of manufacturable three-dimensional composites with multifunctional characteristics

S. Torquato,[a] S. Hyun, and A. Donev
Princeton Materials Institute and Department of Chemistry, Princeton University, Princeton, New Jersey 08544

(Received 27 June 2003; accepted 29 July 2003)

We present an optimization method to design three-dimensional composite microstructures with multifunctional characteristics. To illustrate the fascinating types of microstructures that can arise in multifunctional optimization, we apply our methodology to the study the simultaneous transport of heat and electricity in three-dimensional, two-phase composites. We assume that phase 1 has a high thermal conductivity but low electrical conductivity and phase 2 has a low thermal conductivity but high electrical conductivity. The objective functions consist of different combinations of the dimensionless effective thermal and electrical conductivities. When the sum of the effective thermal and electrical conductivities is maximized, we find that the optimal three-dimensional microstructures are triply periodic bicontinuous composites with interfaces that are the Schwartz primitive (P) and diamond (D) minimal surfaces. Maximizing the effective thermal conductivity and minimizing the effective electrical conductivity results in a special dispersion of inclusions in a connected matrix. The effective properties of both the bicontinuous and singly connected microstructures lie on known optimal cross-property bounds. When the sum of the effective thermal and electrical conductivities is minimized, the result is the three-dimensional checkerboard, which is the optimal single-scale microstructure. It is important to note that current fabrication techniques enable one to manufacture all of the aforementioned optimal single-scale composites. © *2003 American Institute of Physics.* [DOI: 10.1063/1.1611631]

I. INTRODUCTION

A variety of performance demands are increasingly being placed on material systems. The current trend to develop such multifunctional materials has been further fueled by progress in our ability to synthesize materials and to design and analyze materials via computer simulations. Multifunctional requirements include component structures that have desirable mechanical, thermal, electromagnetic, chemical, and flow properties, and low weight.[1–3] Desirable mechanical properties include stiffness, ductility, and strength. Useful thermal properties include high thermal conductivity to dissipate heat and thermal expansion characteristics that match the attached components. In the case of porous cellular solids, heat dissipation can be improved by forced convection through the material, but in these instances the fluid permeability of the porous material must be large enough to minimize power requirements for convection. It is difficult to find single homogeneous materials that possesses these multifunctional characteristics.

Composite materials are ideally suited to achieve multifunctionality since the best features of different materials can be combined to form a material that has a broad spectrum of desired properties. The ultimate multifunctional materials are provided by nature; virtually all biological material systems are composites that typically are endowed with a superior set of properties. This is clearly due to the fact that biological systems must be able to perform a variety of functions well, i.e., roughly speaking, biological materials are ''optimized'' for multifunctional purposes. Currently, there are only a few examples that rigorously demonstrate the effect of competing property demands on synthetic composite microstructures. The purpose of this article is to find additional examples using first principles (cross-property relations and the numerical topology optimization method, as explained below) and develop insights about these intriguing optimal microstructures.

In the most general situation, it is desired to design a composite material with N different effective properties, which we denote by $K_e^{(1)}, K_e^{(2)}, \ldots, K_e^{(N)}$, given the individual properties of the phases. In principle, we would like to know the region (set) in the multidimensional space of effective properties in which all composites must lie (see Fig. 1). The size and shape of this region depends on how much information about the microstructure is specified and on the prescribed phase properties. For example, the set in which even the volume fractions are not specified is clearly larger than the one in which the volume fractions are specified. The determination of the allowable region is generally a highly complex problem. However, the identification of the allowable region can be greatly facilitated if *cross-property* bounds on the effective properties can be found. Cross-property bounds are inequalities that rigorously link different effective properties to one another. For example, links between different transport properties[4–8] and between the conductivity and elastic moduli[9,10] have been established. When cross-property bounds are optimal (i.e., the best possible

[a]Author to whom correspondence should be addressed; electronic mail: torquato@princeton.edu

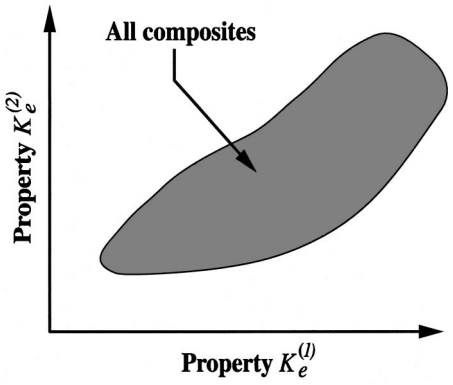

FIG. 1. Schematic illustrating the allowable region in which all composites with specified phase properties must lie for the case of two different effective properties.

bounds), they can be used to identify the boundary of the allowable region. Numerical optimization methods[11–18] can subsequently be employed to discover the specific composite microstructures that lie on the boundary.

In this article, we adapt the topology optimization method[11,12,14,15,18] for the multifunctional optimization of three-dimensional composites. With a few exceptions,[18,19] the topology optimization technique has primarily applied to extremize a *single* effective property. To illustrate our methodology, we consider the optimization involving two different effective properties for three-dimensional, two-phase composites: scalar effective electrical conductivity σ_e and scalar effective thermal conductivity λ_e.

By mathematical analogy, all of our results apply to any of the pair of the following scalar effective properties: electrical conductivity, thermal conductivity, dielectric constant, and magnetic permeability. Thus, for example, our results apply to the maximization of mass transport and flow of electricity; an optimization problem of relevance for intercalation cathodes in batteries.[20]

We consider cases in which phase 1 has a high thermal conductivity but low electrical conductivity and phase 2 has a low thermal conductivity but high electrical conductivity. The objective functions consist of different combinations of the effective thermal and electrical conductivities. When the sum of the effective thermal and electrical conductivities is maximized, we find that the optimal three-dimensional microstructures are bicontinuous triply periodic minimal surfaces. These results were first reported in a short communication,[19] but here we provide details that were not given there. Maximizing the effective thermal conductivity and minimizing the effective electrical conductivity results in a special dispersion of inclusions in a connected matrix. The effective properties of both the bicontinuous and singly connected microstructures lie on known optimal cross-property bounds.[4,5] When the sum of the effective thermal and electrical conductivities is minimized, the result is the three-dimensional checkerboard, which is the optimal single-scale microstructure. It is noteworthy that current fabrication techniques enable one to manufacture all of the aforementioned optimal single-scale composites.[21–23]

In Sec. II, we review previous work on rigorous single-property bounds and cross-property bounds between the electrical and thermal conductivities of three-dimensional composites. In Sec. III, our general numerical procedure for multifunctional optimization is described. In Sec. IV, we present the optimized microstructures that we find for various objective functions involving the electrical and thermal conductivities and compare our results to cross-property bounds. Concluding remarks are given in Sec. V.

II. RIGOROUS BOUNDS AND CROSS-PROPERTY RELATIONS

A. Hashin–Shtrikman bounds

Consider a three-dimensional isotropic composite material that consists of phase 1 with conductivity σ_1 and volume fraction ϕ_1 and phase 2 with conductivity σ_2 and volume fraction $\phi_2(=1-\phi_1)$. The effective conductivity σ_e of the composite is bounded by the Hashin–Shtrikman (HS)[24] bounds, which are given by

$$\langle\sigma\rangle-\frac{\phi_1\phi_2(\sigma_1-\sigma_2)^2}{\langle\tilde{\sigma}\rangle+2\sigma_{\min}}\leqslant\sigma_e\leqslant\langle\sigma\rangle-\frac{\phi_1\phi_2(\sigma_1-\sigma_2)^2}{\langle\tilde{\sigma}\rangle+2\sigma_{\max}}, \tag{1}$$

where

$$\langle\sigma\rangle=\sigma_1\phi_1+\sigma_2\phi_2, \quad \langle\tilde{\sigma}\rangle=\sigma_1\phi_2+\sigma_2\phi_1, \tag{2}$$

and $\sigma_{\min}$ and $\sigma_{\max}$ denote the smallest and largest phase conductivities, respectively. Because of mathematical analogy, these bounds for the electrical conductivity translate immediately into equivalent bounds for the effective thermal conductivity, dielectric constant, magnetic permeability, and diffusion coeffient.

The HS bounds are the best bounds (i.e., optimal) on the effective conductivity given only the volume fractions and the phase conductivities because they are known to be attainable by several different types of structures. These attainable structures include certain multi-scale structures, such as space-filling singly-coated spheres[24] and hierarchical laminates.[25,26] Moreover, in two dimensions, Vigdergauz[27] has shown that there is a special dispersion of single-scale inclusions in a connected matrix that realize the two-dimensional HS bounds. The three-dimensional analogue of the two-dimensional single-scale Vigdergauz structures[27] most likely realize the HS bounds, although this has not been proved rigorously yet. In Sec. IV, we provide numerical evidence that Vigdergauz-like dispersions realize the three-dimensional HS bounds.

B. Cross-property relations

When multiple properties, e.g., transport properties, elastic moduli, permeability, and diffusion coefficient are to be determined in a composite material, one can utilize cross-property relations to estimate one property easily from another one.[3–10] These physical characteristics are rigorously linked to each other because these properties reflect the morphological information about the heterogeneous media. The cross-property relations are especially useful if one property is more easily measured than the other properties.

Consider a two-phase composite material in which phase i has electrical conductivity σ_i, thermal conductivity λ_i, and volume fraction ϕ_i, where $i=1$ or 2. Cross-property bounds exist between the effective electrical conductivity σ_e and thermal conductivity λ_e. Bergman[4] derived the following cross-property bounds:

$$\frac{\lambda_2-\lambda_1}{\lambda_e-\phi_1\lambda_1-\phi_2\lambda_2}-\frac{\sigma_2-\sigma_1}{\sigma_e-\phi_1\sigma_1-\phi_2\sigma_2}=\frac{3(\lambda_2\sigma_1-\sigma_1\sigma_2)}{\phi_1\phi_2(\lambda_2-\lambda_1)(\sigma_2-\sigma_1)}, \tag{3}$$

$$\frac{\tilde{\lambda}_2-\tilde{\lambda}_1}{\tilde{\lambda}_e-\phi_1\tilde{\lambda}_1-\phi_2\tilde{\lambda}_2}-\frac{\tilde{\sigma}_2-\tilde{\sigma}_1}{\tilde{\sigma}_e-\phi_1\tilde{\sigma}_1-\phi_2\tilde{\sigma}_2}=\frac{3(\tilde{\lambda}_2\tilde{\sigma}_1-\tilde{\lambda}_1\tilde{\sigma}_2)}{\phi_1\phi_2(\tilde{\lambda}_2-\tilde{\lambda}_1)(\tilde{\sigma}_2-\tilde{\sigma}_1)}, \tag{4}$$

where $\tilde{\sigma}\equiv 1/\sigma$ and $\tilde{\lambda}\equiv 1/\lambda$. Relation (3) gives an upper (lower) bound and relation (4) gives a lower (upper) bound when the sign of

$$\frac{\lambda_2\sigma_1-\lambda_1\sigma_2}{\sigma_1-\sigma_2} \tag{5}$$

is positive (negative). By employing the three-dimensional phase-interchange inequality

$$\frac{\sigma_e(\sigma_1,\sigma_2)\sigma_e(\sigma_2,\sigma_1)}{\sigma_1\sigma_2}+\frac{\sigma_e(\sigma_1,\sigma_2)+\sigma_e(\sigma_2,\sigma_1)}{\sigma_1+\sigma_2}\geqslant 2, \tag{6}$$

Milton[5] conjectured and Avellaneda *et al.*[6] proved that the aforementioned lower bound [when Eq. (5) is positive] for isotropic media can be improved by

$$\frac{\sigma_1+2\sigma_2}{\sigma_1-\sigma_2}\left(\frac{\sigma_2+2\sigma_1}{\sigma_1-\sigma_2}-\phi_2\frac{\sigma_e+2\sigma_1}{\sigma_1-\sigma_e}\right)=\frac{\lambda_1+2\lambda_2}{\lambda_1-\lambda_2}\left(\frac{\lambda_2+2\lambda_1}{\lambda_1-\lambda_2}-\phi_2\frac{\lambda_e+2\lambda_1}{\lambda_1-\lambda_e}\right). \tag{7}$$

We note that such cross-property relations have been generalized to treat any number of phases.[28]

The bound Eq. (7) is optimal because it is realizable by doubly-coated spheres, which degenerate to the HS singly-coated spheres when one of the coating thicknesses is zero. For doubly-coated spheres, one phase is always disconnected (except in the trivial instance in which the volume fraction is unity). The reciprocal bound Eq. (3) was shown by Milton to be optimal at five distinct points on this bound. One of these points in the $\sigma_e-\lambda_e$ plane, which we denote by (σ_*,λ_*), corresponds to a special bicontinuous multiscale composite: a polycrystal in which each grain is composed of a laminate consisting of alternating slabs of phases 1 and 2 such that the slab thicknesses are much smaller than the size of the grain and the grains are randomly oriented.[29] The effective conductivities $\sigma_*(\phi_2)$ and $\lambda_*(\phi_2)$ of such a statistically isotropic polycrystal are given by

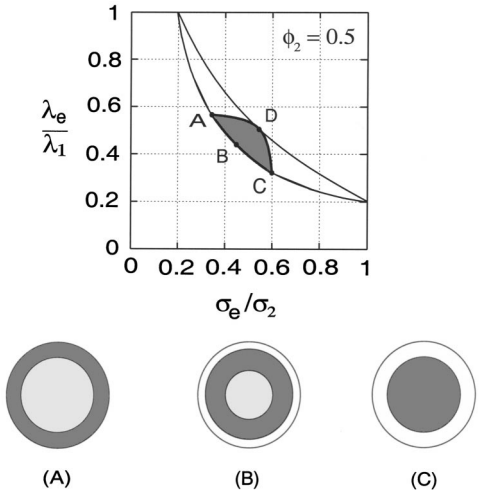

FIG. 2. Cross-property bounds (3) and (7) in the $\sigma_e-\lambda_e$ plane at a volume fraction $\phi_2=\phi_1=1/2$ for a case of ill-ordered phases in which $\sigma_1=0.1$, $\sigma_2=1$, $\lambda_1=1$, and $\lambda_2=0.1$. The basic structural units corresponding to points A, B, and C are shown. Point D is achieved by certain bicontinuous structures. The curves corresponding to the larger lens-shaped region are the cross-property bounds for arbitrary volume fractions for the same choice of phase properties.

$$\sigma_*(\phi_2)=\phi_1\sigma_1+\phi_2\sigma_2-\frac{\phi_1\phi_2(\sigma_2-\sigma_1)^2}{3(\phi_1\sigma_2+\phi_2\sigma_1)},$$
$$\lambda_*(\phi_2)=\phi_1\lambda_1+\phi_2\lambda_2-\frac{\phi_1\phi_2(\lambda_2-\lambda_1)^2}{3(\phi_1\lambda_2+\phi_2\lambda_1)}. \tag{8}$$

We emphasize that this point lies on Bergman's bound.

It is noteworthy that any composite structure corresponding to this point has a three-point microstructural parameter $\zeta_2=1-\zeta_1$, which arises in the Beran three-point bounds on the effective conductivity,[3,8,30] that is exactly given by $\zeta_2=\phi_2$ (or $\zeta_1=\phi_1$). This is easy to verify by comparing the Beran bounds, which are exact through third order in the difference in phase conductivities, to the effective conductivity expression in Eq. (8).

Figure 2 shows the lens-shaped region defined by the cross-property bounds Eqs. (3) and (7) in the $\sigma_e-\lambda_e$ plane at a volume fraction $\phi_2=1/2$ for a case of ''ill-ordered'' phases in which $\sigma_1=0.1$, $\sigma_2=1$, $\lambda_1=1$, and $\lambda_2=0.1$. Points A and C, which define the intersection points of the lower bound and upper bound curves, are realized by the HS singly coated assemblages of spheres and are special limits of the aforementioned doubly coated spheres model, indicated by point B in the figure. Point D on the upper bound corresponds to the aforementioned bicontinuous multiscale composite. The basic structural units corresponding to points A, B, and C are also shown in the figure. We will show below that our multifunctional optimization procedure leads to certain single-scale bicontinuous structures that correspond to point D. We also include in Fig. 2 the corresponding cross-property bounds for arbitrary volume fractions (the larger lens-shaped region), which are obtained by the union of the sets defined by bounds Eqs. (3) and (7) over the volume fractions.

III. OPTIMIZATION TECHNIQUE FOR MULTIFUNCTIONAL DESIGN

To determine the optimal microstructures of heterogeneous media for multiple properties, we utilize the conventional topology optimization technique.[11,12] The topology optimization technique has been used to determine optimal structures without imposing the underlying topology. This feature is very important because the effective properties of a composite depend sensitively on the connectivity of the phases. This technique has been adapted to various types of other optimization schemes, including target optimization.[13,14] To apply this optimization technique for the problem of multifunctional optimization, the objective function will need to be modified, as will be described below.

It is useful to review the salient points behind the standard topology optimization scheme. Consider a composite material that consists of M phases such that each phase is characterized by N material properties. To begin, the design domain is digitized into n finite elements. To simulate infinite systems, we consider a simple unit domain with periodic boundary conditions. One could begin by making an initial guess for the distribution of the phases among the elements, solve for the local fields using finite elements, homogenize, and then evolve the microstructure to the optimal configuration. However, even for a small number of elements, this integer-type optimization problem becomes a huge and intractable combinatorial problem.

Following the idea of standard topology optimization procedures, we relax the problem by allowing the material at a given point to be a gray-scale mixture of the phases.[12,31] In the relaxed system, we let $x_\alpha^i \in [0,1]$ be the local density of phase α ($\alpha=1,2,...,M$) in the ith element, so that when $x_\alpha^i = 0$, the element is devoid of phase α and when $x_\alpha^i = 1$, the element is entirely phase α. Let $\mathbf{x}$ (x_α^i; $i=1,...,n, \alpha = 1,...,M$) be the vector of design variables which satisfies the constraints for the fixed phase volume fractions $\phi_\alpha = \Sigma_{i=1}^n x_\alpha^i/n$ such that $\Sigma_{\alpha=1}^M \phi_\alpha = 1$. Let $\mathbf{K}$ ($K_\alpha^{(j)}$; $j = 1,...,N, \alpha = 1,...,M$) be the tensor of material properties of the phases. For any $\mathbf{x}$, the local fields are computed using the finite element method and the effective property $K_e^{(j)}(\mathbf{x})$, which is a function of the densities $\mathbf{x}$ and of course depends on the individual material properties $\mathbf{K}$, is obtained by the homogenization of the local fields. Here we assume that the composite is macroscopically isotropic and it is implicitly assumed that the scalar effective properties $K_e^{(j)}(\mathbf{x})$ ($j=1,...,N$) have been appropriately made dimensionless.

For the optimization problem involving multiple properties ($K_e^{(j)}$; $j=1,...,N$), we take the objective function Φ to be the weighted average of the effective properties. The multifunctional optimization problem is defined as follows:

$$\max_{\mathbf{x}}: \quad \Phi = \sum_{j=1}^{N} w_j K_e^{(j)}(\mathbf{x}), \tag{9}$$

$$\text{subject to:} \quad \frac{1}{n}\sum_{i=1}^{n} x_\alpha^i = \phi_\alpha, \quad \alpha = 1,...,M$$

$$\sum_{\alpha=1}^{M} x_\alpha^i = 1, \quad i = 1,...,n$$

$$x_\alpha^i \geqslant 0, \quad i = 1,...,n, \quad \alpha = 1,...,M$$

and prescribed symmetries.

Here w_j is the weighting factor associated with the jth effective property $K_e^{(j)}$. Clearly, changing the weighting factors changes the objective function. A higher positive weighting factor can be assigned when some property is deemed to be of greater importance in the optimization problem. A negative weighting factor is used when the corresponding property is to be minimized.

The objective function Φ is generally nonlinear. It can be linearized by expanding $K_e^{(j)}(\mathbf{x})$ in Taylor series around a given microstructure $\mathbf{x}_0$:

$$K_e^{(j)}(\mathbf{x}) \simeq K_e^{(j)}(\mathbf{x}_0) + \nabla K_e^{(j)} \cdot \Delta\mathbf{x}, \tag{10}$$

where $\Delta\mathbf{x} = \mathbf{x} - \mathbf{x}_0$ is the vector of density changes. Thus, the objective function is given by

$$\Phi \simeq \Phi(\mathbf{x}_0) + \sum_{j=1}^{N} w_j \nabla K_e^{(j)} \cdot \Delta\mathbf{x}. \tag{11}$$

This linearized objective function enables us to take advantage of powerful sequential linear programming techniques. In each iteration, the microstructure evolves to the optimal state by determining the *small* change $\Delta\mathbf{x}$. In each iteration, the homogenization step to obtain the effective property $K_e^{(j)}(\mathbf{x}_0)$ is carried out numerically via the finite-element method on the given configuration $\mathbf{x}_0$. Derivatives of the effective material properties ($\nabla K_e^{(j)}$) are calculated by a sensitivity analysis which requires a finite element calculation for each property. Towards the end of the simulation, penalizations are implemented so that x_α^i takes on the binary values zero or unity. The reader is referred to Sigmund and Torquato for additional details regarding the topology optimization method.[12] Here we follow Hyun and Torquato[14] by using the interior point method[32] to solve the linear program as opposed to the simplex method used in Ref. 12.

For concreteness, we illustrate the multifunctional optimization method by considering a three-dimensional two-phase composite that is characterized by two scalar effective properties, namely, the effective thermal conductivity λ_e, and effective electrical conductivity σ_e. The objective function for ill-ordered phases ($\sigma_1 > \sigma_2, \lambda_1 < \lambda_2$) becomes

$$\Phi = w_1 \frac{\lambda_e(\mathbf{x})}{\lambda_1} + w_2 \frac{\sigma_e(\mathbf{x})}{\sigma_2}. \tag{12}$$

We selected four different objective functions as follows: (1) when the weighting factors are $w_1 = w_2 = 1$, both properties are maximized; (2) when the weighting factors are $w_1 = 1$, $w_2 = -1$, the thermal conductivity is maximized but the electrical conductivity is minimized; (3) when the weighting factors are $w_1 = -1$, $w_2 = 1$, the thermal conductivity is minimized but the electrical conductivity is maximized; and (4) when the weighting factors are $w_1 = w_2 = -1$, both properties are minimized.

The unit domain was chosen to be a cube and was digitized by small cubic finite elements ($80\times80\times80$). Geometric symmetry (threefold-reflection symmetry) was imposed to ensure isotropy of the effective conductivity tensors. This makes the effective domain $20\times20\times20$ voxels.

IV. RESULTS

All of our multifunctional optimizations were carried out at a volume fraction $\phi_1=\phi_2=1/2$. We considered a case of ill-ordered phases in which

$$\sigma_1=0.1, \quad \sigma_2=1.0, \quad \lambda_1=1.0, \quad \lambda_2=0.1. \tag{13}$$

Thus, phase 1 has a high thermal conductivity but low electrical conductivity and phase 2 has a low thermal conductivity but high electrical conductivity. We examined four different sets of weighting factors w_1, w_2 and therefore four different objective functions. However, two of these objective functions lead to the same structures but with the phases interchanged. Once the structures were determined, we then directly computed the effective electrical and thermal conductivities for a case in which the composite possesses well-ordered phases such that

$$\sigma_1=0.02, \quad \sigma_2=1.0, \quad \lambda_1=0.01, \quad \lambda_2=1.0. \tag{14}$$

A. Ill-ordered phases

We found various classes of optimal microstructures achieving the cross-property bounds for specified optimality conditions. Depending on the values of the weighting factors, we found three different types of optimal microstructures: bicontinuous, Vigdergauz-type, and checkerboard structures. Interestingly, the bicontinuous microstructures (which do not exist in two dimensions) maximize both the electrical and thermal conductivities for ill-ordered phases.

1. Bicontinuous structures: Minimal surfaces

First, we took the objective function to be given by $\lambda_e+\sigma_e$ (where $\lambda_1=\sigma_2=1$), i.e., we maximized both properties with same weighting factors ($w_1=w_2=1$). Demanding that the sum of the effective thermal and electrical conductivities is maximized sets up a *competition* between the two effective properties. We find that the optimal result is a bicontinuous composite, as shown in Fig. 3. A *bicontinuous* composite is one in which both phases are connected across the sample. This topological feature (i.e., percolation of both phases) is rare in two dimensions and therefore virtually unique to three dimensions.[3] Bicontinuity allows the structure to maximize both properties for the case of ill-ordered phases. The morphology of both phases in this structure are identical (see Figs. 4 and 5), although at first glance they do not appear to be so. (A shift of the unit cell of Fig. 4 by half of the unit cell length in all directions leads to the unit cell of Fig. 5.) Note that this bicontinuous structure achieves the datum (within small numerical error) shown in Fig. 8 for the cross-property upper bound on the sum of the two conductivities in which $\lambda_e=\sigma_e=0.427$. Although we have fixed the volume fraction at $\phi_1=\phi_2=1/2$, the topological property of bicontinuity will extend to other volume fractions.

FIG. 3. A bicontinuous optimal structure at $\phi_1=\phi_2=1/2$ corresponding to maximization of the sum of the effective electrical and thermal conductivities ($\sigma_e+\lambda_e$) for ill-ordered phases in which $\sigma_1=0.1$, $\sigma_2=1$, $\lambda_1=1$, $\lambda_2=0.1$. Shown is a $2\times2\times2$ unit cell.

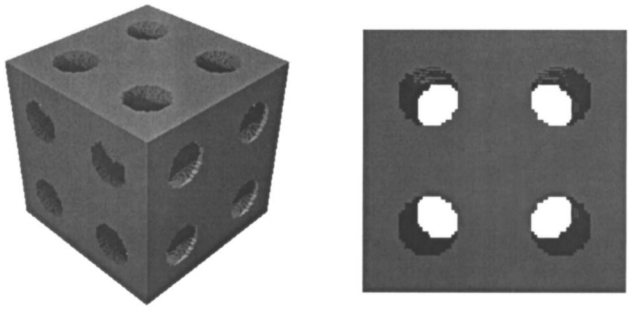

FIG. 4. Morphology of phase 1 ($\sigma_1=0.1$, $\lambda_1=1.0$) viewed at different angles.

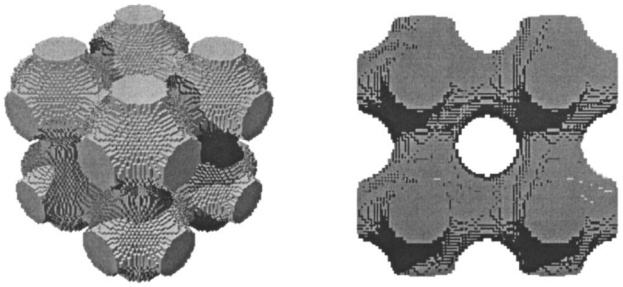

FIG. 5. Morphology of phase 2 ($\sigma_2=1.0$, $\lambda_2=0.1$) viewed at different angles.

Based on visual inspection of the optimal structure produced via the topology optimization method, we hypothesized that the bicontinuous structure is a Schwartz primitive (P) surface, a well-known triply periodic minimal surface with simple cubic symmetry. To verify that this indeed is a Schwartz P minimal surface, we must find an exact representation of it and then compute its effective properties. Minimal surfaces can be characterized exactly using a Weierstrass (complex integration) representation, but in practice this is difficult to use numerically. Instead, we utilized a Landau free-energy type model[33] to calculate numerically a discretization of a potential $\psi(x)$ such that $\psi(x)>0$ for points in

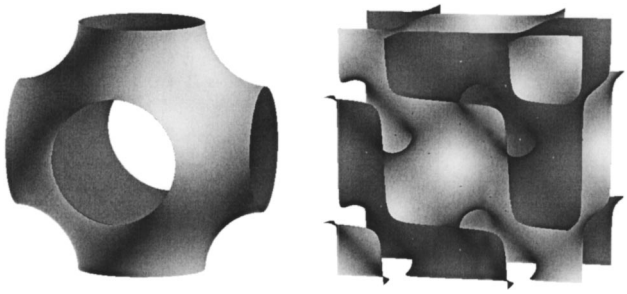

FIG. 6. Unit cells of two different minimal surfaces: (left) Schwartz simple cubic surface and (right) Schwartz diamond surface.

phase 1 and $\psi(x)<0$ for points in phase 2. At the phase interface, $\psi(x)=0$, which in this case is a Schwartz *P* minimal surface.

We obtained the data for this potential (from the authors of Ref. 33) on a 64^3 unit cell as well as one for another minimal surface with macroscopically isotropic effective conductivities, namely, the Schwartz diamond (*D*) surface (see Fig. 6). From these potentials, one can readily make discretizations of bicontinuous two-phase composites having a minimal surface as the two-phase interface boundary. We then used a finite-element code to calculate numerically the effective conductivities of these composites. Remarkably, we found that the computed conductivities for both Schwartz *P* and *D* surfaces matched the ones predicted by the cross-property upper bound up to three decimal places for case (13). Importantly, we also computed the effective conductivities for a wide range of phase contrasts, including the infinite-contrast case ($\sigma_1/\sigma_2\to 0$, $\lambda_1/\lambda_2\to\infty$) and found the same agreement with the corresponding analytical results. This provides strong evidence that these minimal surfaces indeed realize the upper bound (within numerical error), independent of the phase contrast. In light of the discussion at the end of Sec. II, the three-point microstructural parameters for the Schwartz *P* and *D* bicontinuous structures are equal and given by $\zeta_2=\zeta_1=1/2$.

How do minimal surfaces arise when ''surface tension'' is absent in our problem? First, observe that the case examined here represents a special point on the cross-property upper bound (see Fig. 2). The phase volume fractions are identical ($\phi_1=\phi_2$) and the dimensionless conductivities are identical ($\sigma_e/\sigma_2=\lambda_e/\lambda_1$). Therefore, the system possesses phase-inversion symmetry, i.e., the morphology of phase 1 is identical to the morphology of phase 2; see Ref. 3 for a more general definition. We also know that if optimal single-scale structures exist, they must be bicontinuous composites. Moreover, in our numerical optimization study, we imposed simple cubic symmetry. In summary, an optimal composite should be bicontinuous, possess phase-inversion symmetry at a volume fraction $\phi_1=\phi_2=1/2$, and possess simple cubic symmetry. The Schwartz *P* surface meets all of these conditions. On the other hand, if we imposed the symmetry of the diamond lattice, we see from our subsequent numerical calculations, we would have expected to find the Schwartz *D* surface. Thus, provided that the composite is macroscopically isotropic at $\phi_1=\phi_2=1/2$, the minimal surface that achieves the point on the upper bound is not unique. A fruitful rigorous approach to proving that these minimal surfaces are indeed optimal would be to use minimum energy principles to develop optimality conditions on the fields and ultimately on the mean curvature of the interface between the phases. Such a study will be the subject of a future article. Note that if one breaks the symmetry of the problem by moving off the point $\phi_1=\phi_2=1/2$, the optimal structure (if it exists) will still be bicontinuous within a neighborhood of $\phi_1=\phi_2=1/2$ but will not be a minimal surface. In future studies, it will be interesting to investigate whether such structures are bicontinuous structures with interfaces of constant mean curvature, which become minimal surfaces at the point $\phi_1=\phi_2=1/2$. Two-phase composites with interfaces of constant mean curvature are also objects of great interest.[34,35]

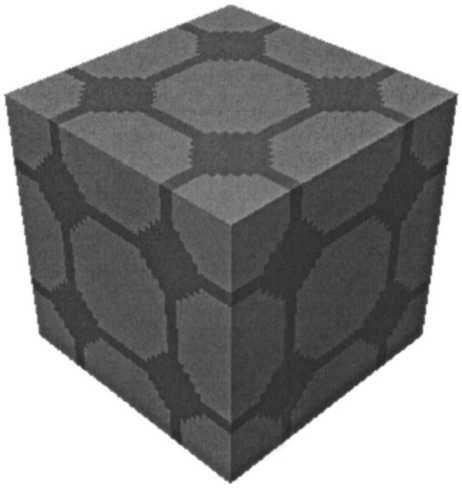

FIG. 7. A three-dimensional Vigdergauz-type dispersion of inclusions in a connected matrix phase at $\phi_1=\phi_2=1/2$ which corresponds to maximization of σ_e and minimization of λ_e for ill-ordered phases in which $\sigma_1=0.1$, $\sigma_2=1$, $\lambda_1=1$, $\lambda_2=0.1$. Shown is a $2\times2\times2$ unit cell. If the phases are interchanged, the same structure minimizes σ_e and maximizes λ_e. It is seen that this structure is virtually optimal for the sum of the conductivities for well-ordered phases in which $\sigma_1=0.02$, $\sigma_2=1.0$, $\lambda_1=0.01$, and $\lambda_2=1.0$ (see Fig. 10).

A remark is in order concerning the analogous ''optimization'' problem in two dimensions. For the ill-ordered case defined by Eq. (13) at $\phi_1=\phi_2=1/2$, the analogous two-dimensional cross-property bounds[5] collapse on to a single curve. Indeed, the same collapse occurs for the more general situation $\lambda_1/\lambda_2=\sigma_2/\sigma_1$ and $\phi_1=\phi_2=1/2$. Thus, the effective properties are uniquely determined and there is no room for optimization.

2. Vigdergauz-type structures

When the objective function is given by the sum $(\lambda_e-\sigma_e)$ or $(\sigma_e-\lambda_e)$, we found three-dimensional generalizations of the two-dimensional Vigdergauz.[27] In the first case, the thermal conductivity is maximized and electrical conductivity is minimized $(w_1=1,w_2=-1)$, and the resulting structure is shown in Fig. 7. The effective electrical conductivity σ_e is given by 0.4706 and the effective thermal conductivity λ_e is given by 0.2940. In the second case, the thermal conductivity is minimized and electrical conductivity is maximized $(w_1=-1,w_2=1)$, and the resulting struc-

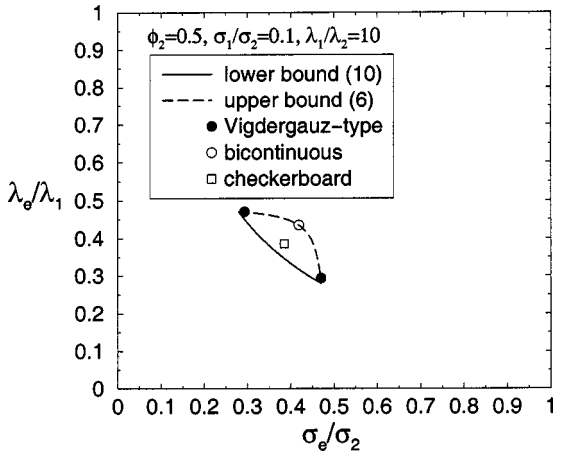

FIG. 8. Cross-property bounds and simulation data for the effective electrical σ_e and thermal λ_e conductivities for ill-ordered phases ($\sigma_1/\sigma_2<1$ and $\lambda_1/\lambda_2>1$) as specified by Eq. (13).

ture is not shown since it is the phase-interchanged version of Fig. 7. Here σ_e is given by 0.2940 and λ_e is given by 0.4706. Note that these structures reside on the corners of the cross-property bounds corresponding to the minimal (maximal) electrical and maximal (minimal) thermal conductivities (Fig. 8). It is not surprising that multifunctional optimization problems reduce here to single property optimizations, i.e., the optimal structures correspond to the HS bounds. Thus, the three-dimensional Vigdergauz structures possess one connected phase and one disconnected phase.

3. Three-dimensional checkerboard

When the objective function is defined by the sum $(-\lambda_e-\sigma_e)$ (i.e., minimizing both properties, $w_1=w_2=-1$), the optimization method did not find any microstructure exactly realizing the lower cross-property bound. Nevertheless, the optimized structures in the intermediate steps suggest that the three-dimensional checkerboard pattern (as shown in Fig. 9) could be the best obtainable single-scale structure to minimize both conductivities. The computed effective electrical conductivity σ_e (equal to the effective thermal conductivity λ_e) of the three-dimensional checkerboard is given by 0.3893. This value is to be compared to the cross-property lower bound of 0.3655 for the arithmetic average of the two effective conductivities [i.e., $(\sigma_e+\lambda_e)/2$].

B. Well-ordered phases

Utilizing the optimized structures obtained above, we then directly computed σ_e and λ_e for the well-ordered case defined by Eq. (14). These results are summarized in Fig. 10.

Not surprisingly, the Vigdergauz-type structures of Fig. 7 (in which only one phase is connected) achieve the upper and lower bounds. For well-ordered phases, the multifunctional optimization problem reduces to a single property optimization, i.e., optimal structures correspond to the HS bounds. It is reasonable to conjecture that the three-dimensional Vigdergauz-type structures exactly realize the HS bounds for the electrical conductivity and thermal conductivity for well-ordered phases. For the case specified by

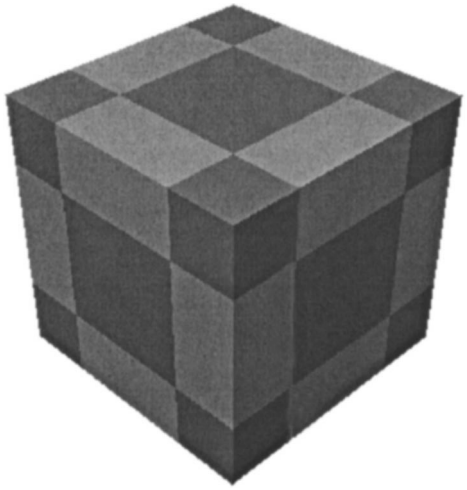

FIG. 9. At $\phi_1=\phi_2=1/2$, the three-dimensional checkerboard is the best single-scale structure that we obtained when both properties are minimized with same weighting factors. Shown is a $2\times2\times2$ unit ce 1. Note that this structure does not achieve the lower bound of the sum of the two conductivities obtained from the cross-property relation (7), as shown in Fig. 8.

Eq. (14), the HS bounds on the electrical conductivity are given by $\sigma_U=0.4137$ and $\sigma_L=0.07614$. The same bounds on the thermal conductivity are given by $\lambda_U=0.4052$ and $\lambda_L=0.03856$. When phase 2 is connected, the computed effective conductivities are given by $\sigma_e=0.4097$ and $\lambda_e=0.4027$. When phase 1 is connected, the computed effective conductivities are given by $\sigma_e=0.08006$ and $\lambda_e=0.04362$. Note that the effective properties for the other two types of optimal structures (bicontinuous structures and checkerboard) lie very close to the cross-property upper bound.

V. CONCLUSIONS

Increasingly, a variety of performance demands are being placed on material systems. Composite materials are ideally suited to achieve multifunctionality since the best features of different materials can be combined to form a material that has a broad spectrum of desired properties.

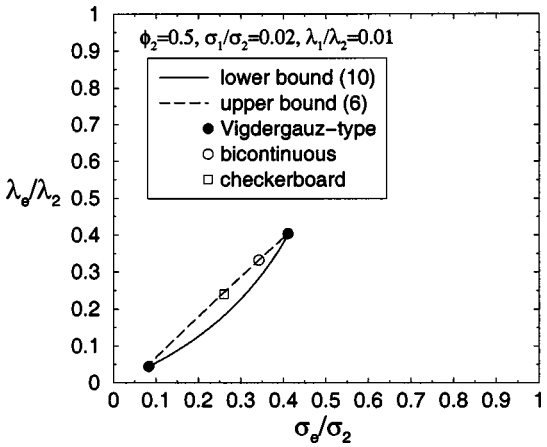

FIG. 10. Cross-property bounds and simulation data for the effective electrical σ_e and thermal λ_e conductivities for well-ordered phases ($\sigma_1/\sigma_2<1$ and $\lambda_1/\lambda_2<1$) as specified by Eq. (14).

Progress in our ability to synthesize composites or porous media at a wide range of length scales and to design and analyze materials via computer simulations is expected to lead to new multifunctional materials.

We have introduced a multifunctional optimization procedure that enables one to identify optimal composite microstructures when the objective function involves a competition between a number of different effective properties. To illustrate the fascinating microstructures that can emerge, we posed several optimization problems involving weighted averages of the dimensionless effective electrical and thermal conductivities for three-dimensional two-phase composites. We examined ill-ordered cases in which phase 1 has a high thermal conductivity but low electrical conductivity and phase 2 has a low thermal conductivity but high electrical conductivity.

When the sum of the effective thermal and electrical conductivities is maximized, we find that the optimal three-dimensional microstructures are triply periodic bicontinuous composites with interfaces that are the Schwartz P and D minimal surfaces. Elsewhere we show that these same triply periodic bicontinuous composites are optimal when a competition is set up between the effective bulk modulus and effective electrical (or thermal) conductivity.[36] These newly discovered extremal properties of triply periodic minimal surfaces may have implications for biology. We have noted that cell membranes resembling periodic minimal surfaces have neen observed in cytoplasmic organelles.[19] It is clear that cell membranes have evolved to allow a variety of different transport processes to occur (e.g., diffusional and electrical) and they must also be stiff enough to act as a structure. Our results[19,36] suggest that it may be fruitful to examine whether the optimization of competing functionalities in biological subsystems can explain their resulting structures.

Maximizing the effective thermal conductivity and minimizing the effective electrical conductivity results in a Vigdergauz-type dispersion of inclusions in a connected matrix. The effective properties of both the bicontinuous and singly connected microstructures lie on known optimal cross-property bounds. When the sum of the effective thermal and electrical conductivities is minimized, the result is the three-dimensional checkerboard, which is the optimal single-scale microstructure. It is noteworthy that current fabrication techniques[21–23] enable one to manufacture all of the aforementioned optimal single-scale composites, and thus such multifunctional bicontinuous materials should find use in a host of applications.

In future studies, we intend to incorporate other effective properties in the multifunctional objective function, including mechanical, flow, chemical, and optical properties. The determination of the optimal microstructures when a competition is set up between these and other properties are intriguing open problems.[36]

ACKNOWLEDGMENTS

The authors are grateful to Graeme Milton for helpful remarks. This work was supported by the MRSEC Grant at Princeton University, No. NSF DMR-0213706 and by the Air Force Office of Scientific Research under Grant No. F49620-03-1-0406.

[1] A. G. Evans, MRS Bull. **26**, 790 (2001).
[2] S. Nemat-Nasser, J. Appl. Phys. **92**, 2899 (2002).
[3] S. Torquato, *Random Heterogeneous Materials: Microstructure and Macroscopic Properties* (Springer-Verlag, New York, 2002).
[4] D. J. Bergman, Phys. Rep. **43**, 377 (1978).
[5] G. W. Milton, J. Appl. Phys. **52**, 5294 (1981).
[6] M. Avellaneda, A. V. Cherkaev, K. A. Lurie, and G. W. Milton, J. Appl. Phys. **63**, 4989 (1988).
[7] S. Torquato, Phys. Rev. Lett. **64**, 2644 (1990); M. Avellaneda and S. Torquato, Phys. Fluids A **3**, 2529 (1991).
[8] G. W. Milton, *Theory of Composites* (Cambridge University Press, New York, 2002).
[9] J. G. Berryman and G. W. Milton, J. Phys. D **21**, 87 (1988).
[10] L. V. Gibiansky and S. Torquato, Phys. Rev. Lett. **71**, 2927 (1993); L. V. Gibiansky and S. Torquato, Proc. R. Soc. London, Ser. A **452**, 253 (1996).
[11] M. P. Bendsoe and N. Kikuchi, Comput. Methods Appl. Mech. Eng. **71**, 197 (1988).
[12] O. Sigmund and S. Torquato, J. Mech. Phys. Solids **45**, 1037 (1997).
[13] A. Diaz and R. Lipton, Struct. Optim. **13**, 6 (1997).
[14] S. Torquato and S. Hyun, J. Appl. Phys. **89**, 1725 (2001).
[15] S. Hyun and S. Torquato, J. Mater. Res. **16**, 280 (2001).
[16] S. Vigdergauz, Int. J. Solids Struct. **38**, 8593 (2001).
[17] T. I. Zohdi, Philos. Trans. R. Soc. London, Ser. A **361**, 1021 (2003).
[18] M. P. Bendsoe and O. Sigmund, *Topology Optimization: Theory, Methods, and Applications* (Springer, New York, 2003).
[19] S. Torquato, S. Hyun, and A. Donev, Phys. Rev. Lett. **89**, 266601 (2002).
[20] C. Julien, in *New Trends in Intercalation Compounds for Energy Storage*, Nato Science Series, edited by C. Julien, J. P. Pereira-Ramos and A. Momchilov (Kluwer, New York, 2002).
[21] L. Yunfeng *et al.*, Nature (London) **410**, 913 (2001); H. Fan, C. Hartshorn, T. Buchheit, D. Tallant, R. Sullivan, S. Torquato, and C. J. Brinker (unpublished).
[22] J. E. Smay, G. M. Gratson, R. E. Shenberd, J. Cesarano, and J. A. Lewis, Adv. Mater. (Weinheim, Ger.) **14**, 1279 (2002).
[23] K. Yu, B. Smarsly, and C. J. Brinker, Adv. Funct. Mater. **13**, 47 (2003).
[24] Z. Hashin and S. Shtrikman, J. Appl. Phys. **33**, 3125 (1962).
[25] G. W. Milton, in *Homogenization and Effective Moduli of Materials and Media*, edited by J. L. Eriksen, D. Kinderlehrer, R. Kohn, and J. L. Lions (Springer, New York, 1986).
[26] G. A. Francfort and F. Murat, Arch. Ration. Mech. Anal. **94**, 307 (1986).
[27] S. B. Vigdergauz, Astrophys. **24**, 57 (1989); S. B. Vigdergauz, J. Appl. Mech. **3**, 300 (1994).
[28] V. Nesi, J. Math. Phys. **32**, 2263 (1991).
[29] K. Schulgasser, J. Math. Phys. **17**, 378 (1976).
[30] M. Beran, Nuovo Cimento **38**, 771 (1965).
[31] M. P. Bendsoe and O. Sigmund, Arch. Appl. Mech. **69**, 635 (1999).
[32] N. Karmarkar, Combinatoria **4**, 373 (1984).
[33] W. T. Gozdz and R. Holyst, Phys. Rev. E **54**, 5012 (1996).
[34] D. M. Anderson, H. T. Davis, L. E. Scriven, and J. C. C. Nitsche, Adv. Chem. Phys. **77**, 337 (1990).
[35] B. Davidovitch, D. Ertas, and T. C. Halsey, arXiv:cond-mat/0210503 (2002).
[36] S. Torquato and A. Donev (unpublished).